DOI: 10.14621/ce.20180102

Predicting Interference Patterns between Offshore Wind Farms through Wake Analysis

Melissa Matis*, Craig G. Merrett, Fred Afagh

Carleton University
K1S 5B6 Ottawa, Canada; melissamatis@cmail.carleton.ca

Abstract

The research is to characterize the wake effect from a cluster of large-scale offshore wind turbines with the purpose of optimizing spacing between separate farms to avoid interference. Placing wind turbines within a field of disturbed flow decreases power output, and in some cases, threatens structural integrity. Unsteady loading and fluxes in wind turbine power generation are born out of turbulence and can further lead to a reduction in the overall energy production of a wind farm. As the offshore wind industry exhibits rapid growth, an immediate need for standards that enable optimization of farm placement for offshore development exists. The wake effect was characterized in the research through computational fluid dynamics (CFD) modelling. ANSYS CFX was used to simulate the wake effects of two proposed offshore wind farms near the shores of Main Duck Island in Lake Ontario, Canada. Additional array simulations were performed to analyse the effect of added rows and increased wind speed on wake recovery length. Three different array configurations were simulated in ANSYS, each containing a different number of rows. The wakes of the 6 x 4 and 7 x 4 arrays had a recovery distance of approximately 13 km. Approximately 89% recovery is achieved at 6.8 km downstream from the 6 x 4 array and at 9 km downstream from the 7 x 4 array. Another simulation was completed using the 7 x 4 array with the inlet wind speed increased by 10%. Results of this simulation revealed a 23% increase in wake recovery length. This research seeks to strategically inform offshore wind farm siting through wake research. Optimizing spacing between wind farms will ultimately maximize power extraction from the excellent offshore wind resources in the Great Lakes region where space is limited.

Keywords:	Offshore wind; Wind farm wake simulations; Computational Fluid Dynamics; Reynolds Averaged Navier-Stokes (RANS) simulation
Article history:	Received: 31 March 2017 Revised: 26 January 2018 Accepted: 26 January 2018

1. Introduction

The purpose of this research was to characterize the cumulative wake effect of large-scale offshore wind turbines in order to optimize spacing between separate farms. The results of this research were submitted for the completion of an M.A.Sc. thesis and to an Ontarian wind energy company that had a vested interest in offshore wind farm development.

Optimized spacing between wind turbines prevents significant power losses incurred from wake-farm interactions. In North America, strategic offshore wind farm development has recently become a priority. An increased volume of potential offshore wind farm sites creates the potential for unwanted interference between farms due to the cumulative wake effects of clusters of wind turbines. Wind speeds and bathometry in several areas of the Great Lakes provide ideal locations for offshore construction; however, it is unknown if these ideal, potential sites lie an adequate distance away from each other in order to avoid interference.

Power losses arise if a single wind turbine's wake impinges on the operation of another turbine. The degree to which energy production is impeded from wind turbine interaction varies as there are multiple factors of influence such as the locations and layouts of wind farms as well as atmospheric stability [1]. A 2007 study found that the energy losses in a downstream turbine can reach nearly 40% due to wake effects and atmospheric stability [2].

High construction costs are often a major roadblock to growth in the offshore wind energy industry; however, offshore wind offers significant advantages over its land counterpart. In addition to the potential for larger power production capacity due to the availability of steadier, stronger winds, many offshore wind farms can be placed close to large cities, reducing the need for extremely long transmission line construction from rural

locations. These benefits, unique to offshore wind, encourage research into optimization of wind farm siting.

Limited studies on the cumulative wake effects of wind farms exist. The vast majority of multi-turbine CFD simulations rely on simplified rotor geometry representations. These simplification techniques require user input source terms that are derived from low-order accurate formulas. Effects of the interactions between a rotor, nacelle, tower and neighbouring turbines are neglected when using simplified geometry [3].

Full rotor geometric representation is the most accurate technique for modelling wind turbine geometry in CFD because it includes the interactions between the turbine blades, tower and nacelle. Comparison studies between the complex full rotor geometry technique and simpler methods have been performed. Réthoré et al. conducted a comparison study between a full rotor, actuator disk and actuator line model. The full rotor simulation was much more computationally expensive than the other models, taking much longer to converge [4]. Another study analysed CFD simulations of the near wake region using a full rotor, actuator disk and actuator line model. The full rotor model captured small structures that have a considerable effect on the development of turbulence which the actuator disk and actuator line models did not predict. This discrepancy may be due to the fact that the inlet condition was not turbulent [5], [6]. Zahle et al. demonstrated good agreement between a single full rotor simulation and experimental data. In this simulation, the rotor's effect on the vortices shed from the tower were successfully captured [7].To date, wind turbine wake simulations which use full rotor representation are often for a single or two turbine case and not for a full array. Also, simulations of wind turbines are often conducted for the purpose of optimization of individual turbine performance.

The next progression in CFD wind turbine research is to simulate entire wind farms to optimize the performance of a cluster of wind turbines. Most multi-turbine CFD simulations use the actuator line or actuator disk rotor representation. In 2014, Scottish research group presented a CFD simulation of the Lillgrund offshore wind farm to validate a time-dependant wind farm model. This simulation modelled the wind turbines using actuator disc methods and employed Large-Eddy solving techniques. Supervisory control and data acquisition (SCADA) data from the Lillgrund wind farm was used for validation of the CFD simulation. The authors present a comparison in wind turbine performance between the CFD simulation and the SCADA data from the wind farm. In some instances the CFD model simulated wind turbine performance well, in other instances the simulation results did not closely match the SCADA data [8].

More recently, an onshore wind farm was simulated by Matias Avila et al. In this work, loaded actuator disks were used to geometrically represent the wind turbines. The purpose of this research was not to analyse the wake extension length of the wind farm, but rather to present a framework for simulating wind farms using an in-house High Performance Computing, RANS-based solving scheme [9].

Research has been done to model entire arrays using the more detailed full rotor geometry representation, but this work is still highly computationally expensive and studies using full rotor modelling techniques for an entire wind farm are scarce. In 2013, a University of Wyoming research group undertook the unprecedented task of simulating a wind farm using full rotor geometry representation. The group had access to large computational resources, allowing them to implement a very fine mesh and a small time step of 0.008 seconds to simulate a 48 turbine array. The University of Wyoming study looked at the intra-farm wake effects rather than the cumulative wake effect of a wind farm and inter-farm wake effects that were analysed in this work. The total convergence time for the 48 turbine simulation was estimated to be 8.5 million core hours [3].

In the work presented in this paper, a full rotor geometric representation was used to simulate the cumulative wake effects of a 24, 28 and 40 turbine array in ANSYS CFX. All simulated turbines were 100 m in diameter and 3 MW in capacity, based upon the Sandia 3 MW blade design [10]. Computational expense was reduced by implementing a larger time step and coarser mesh than what was used in the Wyoming study [3]. These simplifications are rationalized in the methodology section. The 24 and 40 turbine arrays were simulated together in a single domain, spaced 7 km apart. The 28 turbine array simulation was performed separately to analyse the effect of number of rows on wake recovery length. An inlet wind speed sensitivity simulation was also performed on the 28 turbine array using an inlet speed that was increased by 10%. The set-ups of all simulations were informed through CFD theory as well as grid and time step sensitivity analyses. All simulations were run for 800 seconds of physical time, a sufficient amount of time to obtain a solution that remained unchanged for successive iterations with a high level of numerical convergence. Using a 32 core, 128 GB ram cluster, the two-array simulation converged in approximately 26,880 core hours.

2. Theory and methodology

Experimental and numerical methods can be used for wake characterization. There are several drawbacks of

experimental wake characterization of wind turbine clusters. Spatial limitations imposed by wind tunnels limit the number of turbines that can be simulated at a time. Also, spatial limitations and maximum flow rates of wind tunnels limit the Reynolds number that a wind farm can be simulated at to a lower range than what would be common to a full-scale array. Research on the impact of low Reynolds number wake analysis has demonstrated delayed vortex pairing and unnatural narrowing of downstream wakes compared to wake flow in full-scale arrays [11]. Additionally, most wind tunnels are constructed with a material rougher than water, making it difficult to represent the aquatic environment of an offshore wind farm.

These experimental limitations for wind farm wake characterization can be overcome through CFD. Domain sizes in CFD are not constrained to the extent of experimental labs, and can be as large as computational resources allow. The aforementioned wake narrowing that can occur in wind tunnel testing can be avoided through the use of user defined boundary conditions (e.g. openings to the atmosphere and symmetrical boundary conditions). Another benefit of CFD is that the aquatic environment can be included in the simulation through user defined boundary conditions. As such, CFD numerical modelling was used in this research to simulate the offshore arrays. The methodology employed to simulate the offshore arrays in ANSYS CFX is described in this section along with the theory behind the methods used.

2.1. Numerical model approach

Turbulent flow regimes behave chaotically and possess large and small scale motions, all of which must be captured in flow simulations. Velocity and pressure parameters rapidly fluctuate in highly turbulent flow, making it impossible to analytically solve the equations of motion for a Newtonian fluid: the Navier-Stokes (N-S) equations. Through approximations and the use of statistical averaging, the N-S equations can be implicitly solved in CFD. The approximation technique employed in this research was the Reynolds Averaged Navier-Stokes (RANS) model.

In order to close the RANS equations, turbulence models are employed. The *k-ω* SST turbulence model was selected for the simulations. This model is ideal for wind turbine wake simulations as it performs well in adverse pressure gradients and is one of the better models for predicting the onset and amount of flow separation. In the alternative k-ε model, the prediction of flow separation is often delayed or not predicted at all [12]. Wall functions are also important features of turbulence models as they can reduce the need for extremely fine near-wall meshes. Automatic wall functions employed in *ω*-based models allow for arbitrarily fine meshes to be used near the wall, ultimately reducing computation time. An analytical expression is used to resolve the viscous sublayer of the boundary layer (BL) in *ω*-based models, and the logarithmic layer is approximated [13]. Accuracy is reduced in *ε*-based models, because no analytical expressions are used to resolve the viscous sublayer of the BL, and the entire BL is approximated [6]. The superior treatment of near wall flow in *k-ω* SST model further solidified the choice to employ this model in the full-array simulations.

2.2. Simulation mesh

To improve the precision of BL modelling, a biased accumulation of nodes was created in the BL region using fine layers of rectangular elements, normal to the blade surfaces. Tetrahedral elements made up the mesh throughout the rest of the rotational domains which encapsulate the turbine blades, as well as the stationary domain, representative of the offshore environment, nacelles and towers. Figure 1 is an image of a rotational domain containing the wind turbine blades. The darker shading shows the biased accumulation of nodes towards the blades and hub of the wind turbine.

When performing CFD simulations, the first grid point, normal to the wall surface, must lie within the viscous sublayer region of the boundary layer to sufficiently describe the boundary layer. Using fine rectangular elements, normal to the wall aims to place the nodes nearest to the wall in the viscous sublayer. The hybridized mesh surrounding the blades is shown in Figure 2. The degree to which mesh refinement was achieved by creating smaller elements near the blade surface was limited by computational resources and the Courant number. Additionally, the overall parameter of interest in the research is the large scale cumulative

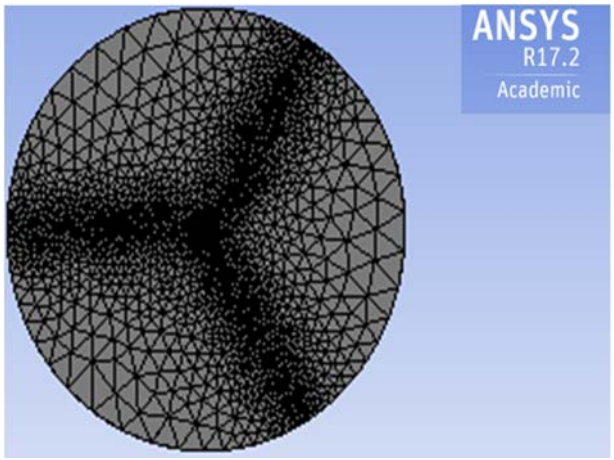

Figure 1 Rotational domain mesh

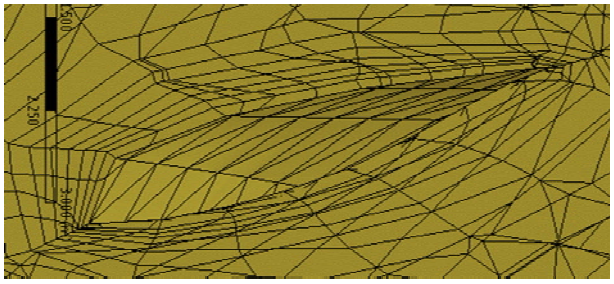

Figure 2. Hybridized mesh surrounding a blade element

Table 1: Grid Convergence Study

Mesh Density Type	Number of Elements
Coarse	355 978
Medium	578 981
Fine	724 988

wake effect, and the flow patterns in the boundary layer were not be studied. In cases like this, full resolution of the boundary layer is not required and so the node density near the wall can be greater than what would be needed to satisfy a Y+ condition of 1 [14]. To compensate for the larger Y+ values, wall functions are implemented by ANSYS CFX to approximate portions of, or all of the boundary layer region. In this treatment of the boundary layer through wall functions, an automatic switch from the low-Reynolds method to wall functions occurs when necessary [15]. Automatic wall functions employed by the k-ω SST turbulence model significantly reduce the mesh size constraints in the boundary layer region, allowing for simulations to be run with an arbitrarily fine near-wall mesh [14].

A single turbine wake was simulated using three different mesh densities to determine the appropriate density that should be employed in the full array simulations. The different densities were created by altering the maximum allowable element spacing in the regions exterior to BL flow, shown in Table 1.

The percent difference in average downstream velocity between the medium and fine simulations was below 1%. Consequentially, the maximum spacing in the mesh outside the BL regions of the full-scale array simulations was set to be the same as the medium mesh density case. The total number of elements in the two-array, full-scale simulation was 48,131,055.

2.3. Simulation time controls and convergence

The nature of the flow regime in the research which includes the behaviour of vortex shedding required the use of transient models. Transient simulations account for the unsteady nature of turbulent flow by allowing the fluid parameters to fluctuate with time [16]. After sufficient run time, a transient simulation will progress towards a steady-state or time-periodic solution [17]. In order to obtain a solution with a wake recovery distance that stopped changing over time, the array simulations in this research had to be run for 800 seconds of physical time. The time step implemented in the simulations was informed through a sensitivity analysis where three different time steps were employed in the simulation of a single 3 MW Sandia rotor design [10]. The three comparison cases used the different time steps of Δt = 0.1 s, 0.2s and 0.4s. At 1300 m downstream from the rotor, the average velocity of all nodes across the rotor diameter was 6.2884 m/s and 6.2878 m/s for the Δt = 0.1 s and Δt = 0.4 s simulations respectively. Percent differences in average velocity across the rotor diameter, at all distances farther downstream from the rotor remained near or under 1%. Because the difference in wake recovery distance between the three simulations was negligible, the largest time step, 0.4 s, was used in the full-scale simulations to reduce computational expense.

The number of iterations needed in a simulation is also determined by the convergence levels of the models. In order to determine convergence levels, the imbalances of the conservation of mass and momentum equations calculated for each control volume of the mesh are measured by the CFD solver at each time step. In ANSYS CFX, the root mean square technique is employed to normalize the imbalances (i.e. the residuals). As the solver progresses through time, the solution should converge if a proper mesh and accurate boundary conditions are employed. Relatively loosely converged solutions have RMS residual levels near 1E-4. This is often a sufficient level for engineering applications. Residual values of 1E-5 are considered well converged and values of 1E-6 are said to be tightly converged [18]. Domain imbalance is also monitored for solution accuracy. Imbalance quantifies the conservation of mass, momentum and energy over the entire domain. In a well converged solution, the total flux entering the domain should be the same as the total flux exiting the domain, with an imbalance of 1% or less [19]. In the offshore array simulations performed in the research, 2000 iterations were required to attain acceptable convergence and domain imbalance levels.

2.4. Simulation boundary conditions

The external sides and the top of the stationary domain were defined as openings with atmospheric pressure. At the cross sectional cut, the symmetry boundary condition was used in ANSYS, as indicated in Figure 2. The symmetry boundary condition assumes that the flow values just adjacent to the domain are the same as the values at the nearest nodes, just inside the domain

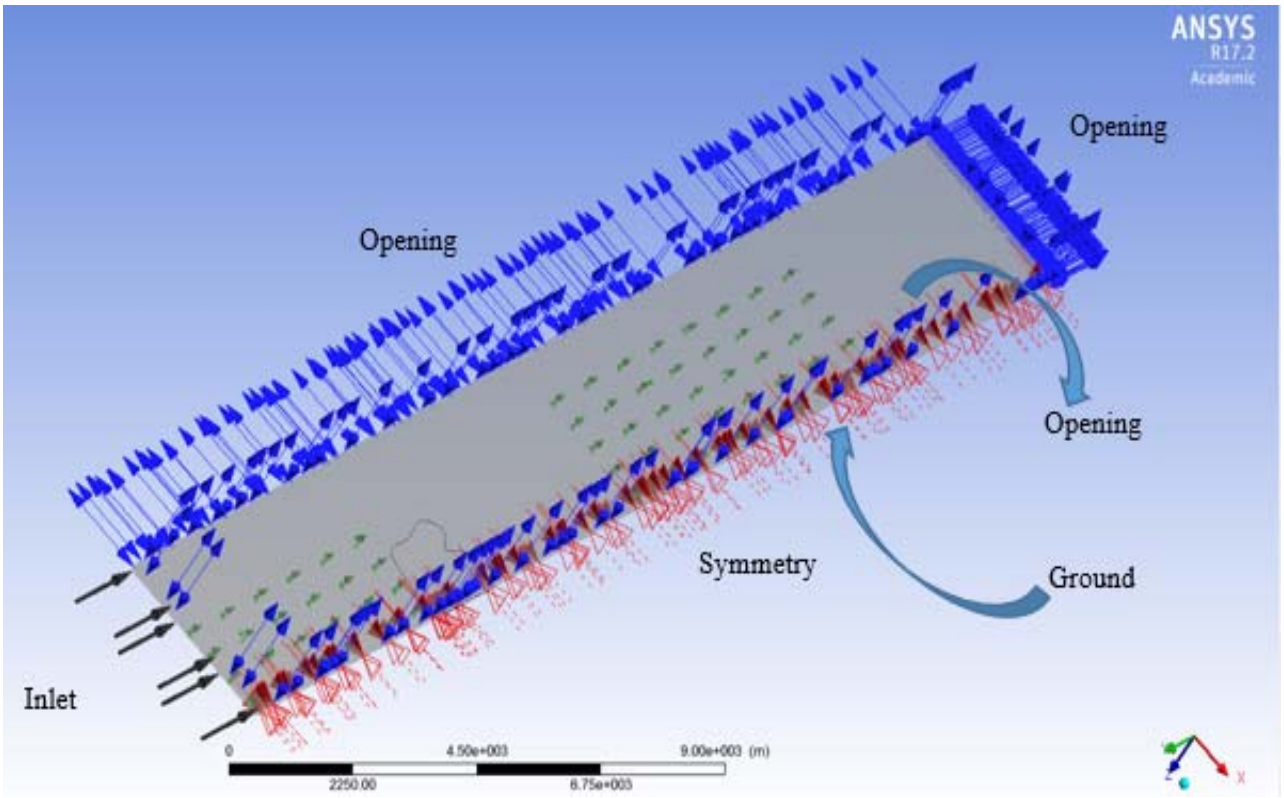

Figure 3. Boundary conditions of the two-array simulation

[20]. To simulate the offshore environment, the bottom plane of the stationary domain was defined as wall with a smooth surface. Turbine blades, nacelles and towers were defined as smooth walls with the no-slip condition. The inlet was defined as a velocity representative of typical weather data gathered at the hub height from the Lake Ontario potential build site. Figure 3 illustrates the location of the aformentioned boundary conditions in the two-array simulation.

The transient rotor stator interface was applied to the boundaries between the rotational wind turbine domains and the stationary domain. The models employed by this interface predict the actual transient interaction of flow through the rotor to the stator [21].

3. Results

The purpose of this research was to study the wake effect of clusters of offshore wind turbines. To do this, two CFD simulations were performed in ANSYS CFX. The first simulation was a two-array simulation based off of two potential build sites in Lake Ontario. To show the effect of number of rows on wake recovery distance, a second CFD simulation was completed with a single 7 x 4 array using the same boundary conditions as the first simulation. The single 7 x 4 array was simulated a second time with an increased inlet wind speed. Results of these CFD simulations are presented in the sub-sections to follow.

3.1. Two-array simulation results (6x4 & 8x5)

For the wake of the 6 x 4 array, the simulation results show that wind velocity is approximately 89% recovered compared to that of the freestream velocity at 6.8 km behind the last row of the array. Figure 4 is a plot of the averaged resultant velocities across the rotor diameters at incremental distances behind the 6 x 4 array.

Figure 5 is a velocity contour plot of the two-array simulation. Stretching and merging of vortex cores results in a re-organization of the overall wake structure. Effects of this re-organization can be seen in Figure 5 through the subtle differences that occurred along the stream wise direction of the wakes. The lateral spreads of the column wakes increased, and meandering periodically occurred in the simulation. Entire wakes of individual columns of turbines periodically drifted to the left due to the motion of large scale eddies in the flow. This drift was followed by a rapid shift back to the right. Bands of significantly increased velocity coincided with the lateral shift of the wakes. Meandering is known to diminish the overall deficit of a wake [22], and could have been the cause of the bands of increased velocity in the simulation. The wake of the leftmost column of

array 2 pictured in Figure 5 was not situated in the wake of Array 1, and so the wake velocity of this column was analysed. The wake recovery rate in this column of the 8 x 5 array was slightly slower than in the 6 x 4 array. At 3 km downstream, the differences in the average wake velocity between the two arrays are pronounced with the 6 x 4 array wake reaching approximately 5.5 m/s and the 8 x 5 array wake reaching approximately 1.8 m/s. However, this difference in velocity deficits between the two arrays became less, farther downstream. At 4.5 km downstream, the average wake velocity in the 5 x 8 array is only 0.4 m/s slower than in the 4 x 6 array at 4.5 km downstream.

Figure 6 plots the turbulent kinetic energy in the wake of a rotor in the sixth row and first column of Array 1. Swells in turbulent kinetic energy precede the surges in velocity present in Figures 4. and 5. Recovery rate of the wake is most rapid from 5000 m to 5500 m downstream of Array 1, as shown in the velocity plot of Figure 4. This trend coincides with a high swell of turbulent kinetic energy near 5000 m. This relationship between turbulent kinetic energy in the flow field with a heightened velocity recovery rate is expected as wake recovery is catalysed by turbulent kinetic energy extracted by large eddies from the mean flow. At 6000 m downstream from the array, where the wake recovery rate is slowed and the velocity deficit is largely recovered, the turbulent kinetic energy has completely dissipated.

3.2. Single array configuration simulation (7x4)

The boundary conditions in the simulation of the 7 x 4 array were the same as in the two-array simulation. Simulation results show that the wind velocity would be completely recovered compared to that of the freestream velocity at approximately 13 km behind the last row of the 7 x 4 array. Figure 7 is a plot of the resultant velocities, normalized over the rotor diameters for increasing distances behind the 7 x 4 array. In this simulation, 89% recovery is achieved at 9 km downstream from the array and from this point forward, wake velocity steadily increases. After 7 km downstream from the array, wake velocity recovery rate is reduced. This is because the large eddies are present further upstream in the wake and are severely dissipated near 6 km downstream; meaning that less mixing would be able to occur to transfer momentum from the freestream into the wake.

3.3. Increased inlet speed for single array simulation (7x4)

The sensitivity of wake recovery length to increased inlet wind speed was analysed for the 7 x 4 array by increasing the inlet wind velocity condition by 10% to 9.66 m/s. All other parameters were kept the same as the 6 x 4 array case. The point in which the average wake velocity was 89% recovered occurred at 10,250 m downstream from the array; 3,450 m farther downstream than the lower inlet speed case. Freestream velocity was regained in the wake near 16 km downstream from the array; 3 km farther than the lower inlet speed case. This is a 23% increase in wake recovery length. As in the cases of the aforementioned array simulations, wake meandering was also present in the increased inlet speed simulation.

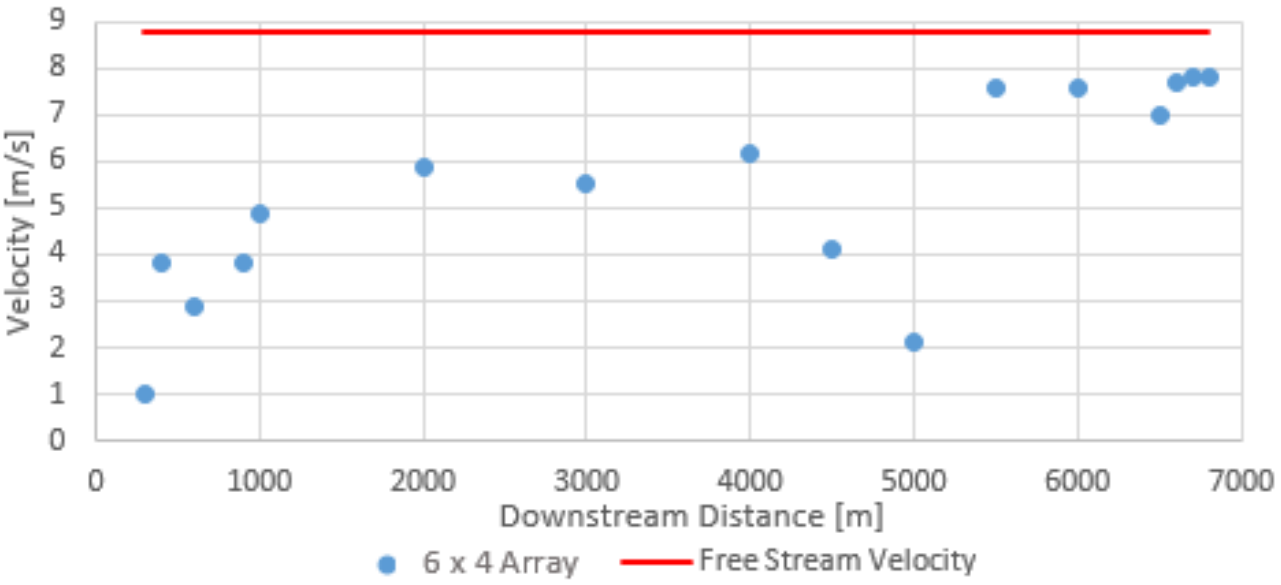

Figure 4. Velocity recovery in a 6 x 4 array wake

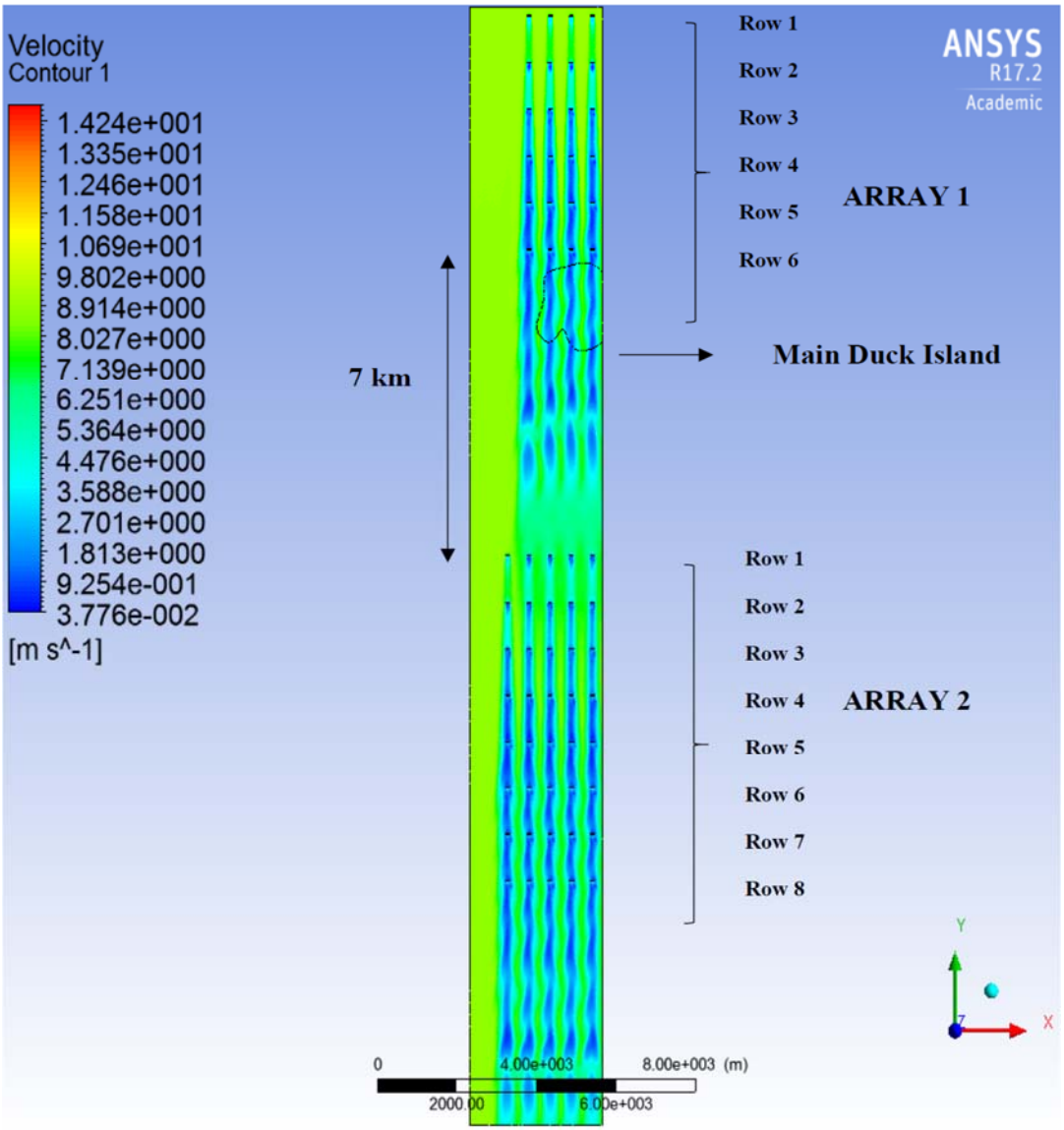

Figure 5. Velocity contour plot of the two-array simulation

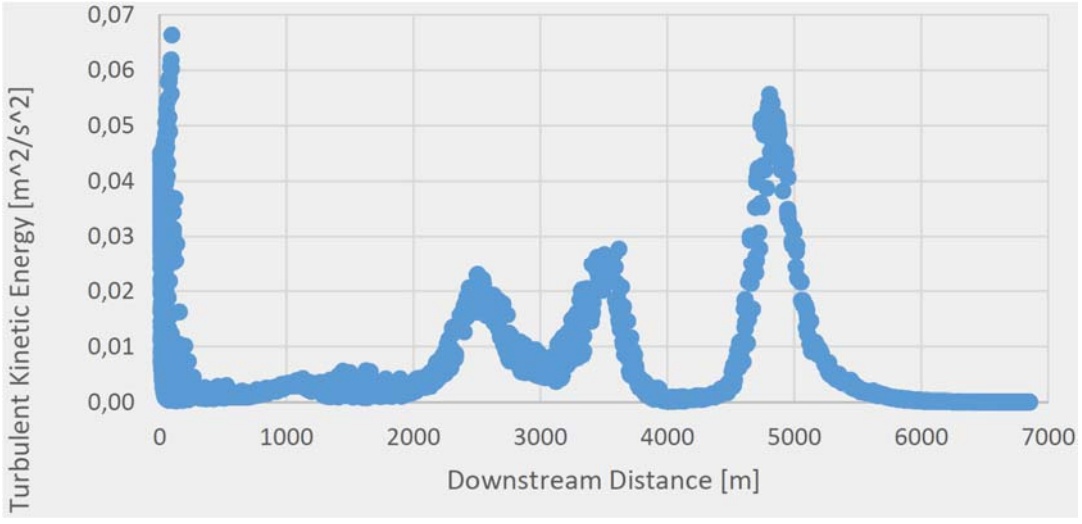

Figure 6. Turbulent kinetic energy in the wake of a single turbine in array 1

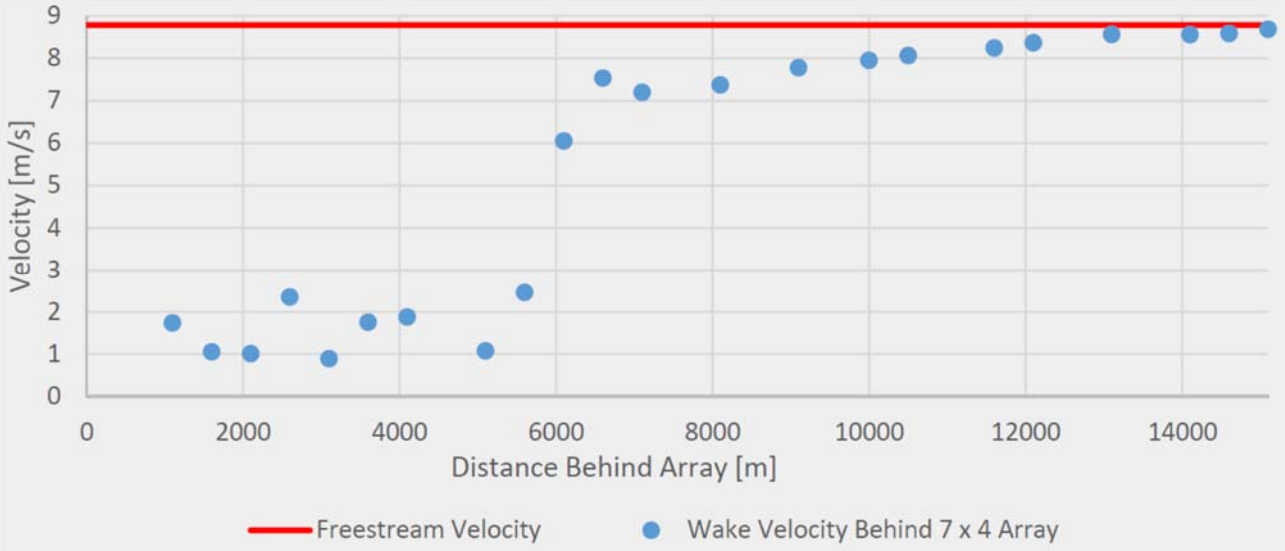

Figure 7. Velocity recovery in a 7 x 4 array wake

Table 2: Residual values and domain imbalance percentages

Rotational Domain Imbalances	Stationary Domain Imbalances	RMS Momentum Residuals	RMS Mass Residuals	RMS k-Turbulence Kinetic Energy	RMS ω-Turbulence Frequency
0.0017%	0.0000016%	1.92E-05	4.22E-06	2.35E-05	9.23E-06

3.4. Convergence levels

In the simulations of this research, the residual values and imbalance percentages indicated that acceptable convergence levels were obtained after 2000 iterations. These values and percentages are specified in Table 2 for the stream wise flow calculations. The same convergence levels and imbalance percentages were attained in the single array simulations and in the mesh and time step sensitivity studies. The residuals and imbalances lie near the ranges of well and tightly converged numerical solutions [23].

4. Conclusion

The offshore array simulations indicate that wake effects are still present in regions far downstream from arrays. This is an important consideration for offshore wind farm development. The two-array simulation revealed that a spacing of 7 km is not quite adequate for the placement of the proposed arrays in the Great Lakes. Freestream velocity levels were estimated to be regained at approximately 13 km downstream from the 7 x 4 array. The wake velocity was largely regained at a significant distance before 13 km in the 6 x 4 and 7 x 4 array simulations (i.e. 89% recovered). At 6.8 km downstream from the 6 x 4 array, and 9 km downstream from the 7 x 4 array, the average wake velocity was approximately 89% of the freestream velocity. The dissipation of large eddies near 6 km downstream of the arrays is attributed to the slowed recovery rate of the velocity deficit after 89% recovery was achieved. The results predicted a 32% increase in wake recovery distance when a row was added to an array.

The increased inlet wind speed simulation revealed that a 10% increase in freestream velocity has a significant impact on wake recovery length. In this comparison study, the inlet speed was increased from 8.78 m/s to 9.65 m/s and the wake velocity returned to freestream levels at approximately 16 km; 3 km further downstream from the point in which the lower inlet speed simulation wake was recovered. Residual RMS values for the array simulations indicated that the final solutions were well converged. Imbalance percentages were also well under the convergence criteria of 1% for the stationary and rotational domains. Sensitivity studies were also used to verify the mesh and time step employed in the simulations. The results of this research can inform offshore wind farm siting to alleviate power losses incurred through wake-farm interactions.

Acknowledgements

The authors gratefully acknowledge Trillium Wind Power and the *Natural Sciences and Engineering Research Council* of Canada for their financial contributions to this work as well as the Programme Committee of REMOO–2017 for efforts done for the success of the event.

References

[1] Z. Wang, "Experimental and Numerical Investigations on the Flow Characteristics of Rotary," *Ph.D. dissertation,Dept. of Aero. Eng., Iowa State University, Ames, IA,* 2015.

[2] R. Barthelmie, S. Frandsen, N. Nielsen, S. Pryor, P. Réthoré and H. Jørgensen, "Modelling and measurements of power losses and turbulence intensity in wind turbine wakes at middelgrunden offshore wind farm," *Wind Energy,* p. 10:217–228, 2007.

[3] W. Miller, J. Sitaraman and D. L. Mavriplis, "Scale Simulations of Wind Farm Aerodynamics in Turbulent Atmospheric Inflow Conditions," University of Wyoming, 2013 .

[4] P. Réthoré, N. Troldborg, F. Zahle and N. Sørensen, "Comparison of the Near Wake of Different Kinds of Wind Turbine CFD Models," *Wake Conference. Gotland,* p. 7, 2011.

[5] R. Mikkelsen, J. Sørensen, S. Øye and N. Troldborg, "Analysis of Power Enhancement for a Row of Wind Turbines Using the Actuator Line Technique," *Journal of Physics: Conference Series 75,* 2007.

[6] B. Johnson, "Computational Fluid Dynamics (CFD) Modelling of Renewable Energy Turbine Wake Interactions, Ph.D. Dissertation, University of Central Lancashire," Preston, England, 2015.

[7] F. Zahle, N. Sørensen and J. Johansen, "Wind turbine rotor-tower interaction using an incompressible overset grid method," *Wind Energy,* vol. 12, no. 6, p. 594–619., 2009.

[8] A. Creech, W.-G. Früh and A. E. Maguire, "Simulations of an offshore wind farm using large eddy simulation and a torque-controlled actuator disc model," *Surveys in Geophysics ,* vol. 36(3), pp. 36-40, 42, 2015.

[9] M. Avila, A. Gargallo-Peir´o and A. Folch, "A CFD framework for offshore and onshore wind," *J. Phys.: Conf. Ser. ,* no. 854 012002, 2017.

[10] Sandia National Laboratories, "Innovative Design Approaches for Large Wind Turbine Blades Sandia Report," WindPACT Blade System Design Studies, Warren, RI, 2003.

[11] S. McTavish, "Identification of Wind Turbine Testing Practices and Investigation of the Performance Benefits of Closely-Spaced Lateral Wind Farm Configurations", Ph.D. dissertation,Dept. of Mech. and Aero. Eng., Carleton University, Ottawa, Ontario, 2013.

[12] F. Menter, "Improved Two-Equation k-ω Turbulence Models for Aerodynamic Flows," NASA AMES Research Center, Moffett Field, California, 1992.

[13] G. Kalitzin, G. Medic, G. Iaccarino and P. Durbin, "Near-wall behavior of RANS turbulence models and implications for wall functions," *Journal of Computational Physics,* pp. 265-291, 2005.

[14] ANSYS®, Academic Research, Release 11.0, ANSYS CFX-Solver Theory Guide, Turbulence and Wall Function Theory , ANSYS, Inc...

[15] ANSYS Inc., "4.2. Modeling Flow Near the Wall," ANSYS ®, Academic Research, Release 15.0, ANSYS CFX-Solver Theory Guide.

[16] ANSYS Inc., "1.2.1. Steady State and Transient Flows," ANSYS ®, Academic Research, Release 15.0, ANSYS CFX-Solver Theory Guide, 2008.

[17] ANSYS® Academic Research, ANSYS 2009, Introduction to CFX, Transient Simulations , ANSYS, Inc..

[18] ANSYS® Academic Research, Release 16.2, Help System, 15.10.1 Residuals, ANSYS, Inc..

[19] ANSYS® Academic Research, ANSYS 2009, Introduction to CFX, Solver Settings , ANSYS, Inc..

[20] ANSYS Help System, Release 16.2, 1.9.7. Symmetry Plane, ANSYS Inc., [Online].

[21] ANSYS® Academic Research, ANSYS 2009, Introduction to CFX, Moving Zones , ANSYS, Inc.

[22] B. Sanderse, "Aerodynamics of Wind Turbine Wakes Literature Review," Energy Research Centre of the Netherlands.

[23] ANSYS® Academic Research, Release 16.2, Help System, 15.10.1 Residuals, ANSYS, Inc..

[24] ANSYS Inc., " Transient Flow Modeling," ANSYS®, Academic Research, Release 13.0,ANSYS CFX-Solver Theory Guide.

[25] ANSYS® Academic Research,Release 15.0, Theory Guide, 2.1.1. Statistical Turbulence Models and the Closure Problem, ANSYS, Inc..

[26] F. Menter, "A comparison of some recent eddy-viscosity turbulence models," Fluids Eng., 1996, pp. 514-519.